remote sensing

MDPI

Article

New Paradigms for Geomorphological Mapping: A Multi-Source Approach for Landscape Characterization

Martina Cignetti, Danilo Godone *, Daniele Ferrari Trecate and Marco Baldo

National Research Council of Italy, Research Institute for Geo-Hydrological Protection (CNR IRPI), 10135 Torino, Italy; martinacarolinaagnese.cignetti@cnr.it (M.C.); danieleferraritrecate@cnr.it (D.F.T.); marco.baldo@cnr.it (M.B.)
* Correspondence: danilofrancescostefano.godone@cnr.it

Abstract: The advent of geomatic techniques and novel sensors has opened the road to new approaches in mapping, including morphological ones. The evolution of a land portion and its graphical representation constitutes a fundamental aspect for scientific and land planning purposes. In this context, new paradigms for geomorphological mapping, which are useful for modernizing traditional, geomorphological mapping, become necessary for the creation of scalable digital representation of processes and landforms. A fully remote mapping approach, based on multi-source and multi-sensor applications, was implemented for the recognition of landforms and processes. This methodology was applied to a study site located in central Italy, characterized by the presence of 'calanchi' (i.e., badlands). Considering primarily the increasing availability of regional LiDAR products, an automated landform classification, i.e., Geomorphons, was adopted to map landforms at the slope scale. Simultaneously, by collecting and digitizing a time-series of historical orthoimages, a multi-temporal analysis was performed. Finally, surveying the area with an unmanned aerial vehicle, exploiting the high-resolution digital terrain model and orthoimage, a local-scale geomorphological map was produced. The proposed approach has proven to be well capable of identifying the variety of processes acting on the pilot area, identifying various genetic types of geomorphic processes with a nested hierarchy, where runoff-associated landforms coexist with gravitational ones. Large ancient mass movement characterizes the upper part of the basin, forming deep-seated gravity deformation, highly remodeled by a set of widespread runoff features forming rills, gullies, and secondary shallow landslides. The extended badlands areas imposed on Plio-Pleistocene clays are typically affected by sheet wash and rill and gully erosion causing high potential of sediment loss and the occurrence of earth- and mudflows, often interfering and affecting agricultural areas and anthropic elements. This approach guarantees a multi-scale and multi-temporal cartographic model for a full-coverage representation of landforms, representing a useful tool for land planning purposes.

Keywords: landform recognition; morpho-evolution description; automated landform classification; Geomorphons; photointerpretation; unmanned aerial vehicle survey; Central Apennine

check for updates

Academic Editor: Takashi Oguchi

Received: 19 November 2024
Revised: 28 January 2025
Accepted: 1 February 2025
Published: 8 February 2025

Citation: Cignetti, M.; Godone, D.; Ferrari Trecate, D.; Baldo, M. New Paradigms for Geomorphological Mapping: A Multi-Source Approach for Landscape Characterization. *Remote Sens.* **2025**, *17*, 581. https://doi.org/10.3390/rs17040581

Copyright: © 2025 by the authors. Licensee MDPI, Basel, Switzerland. This article is an open access article distributed under the terms and conditions of the Creative Commons Attribution (CC BY) license (https://creativecommons.org/licenses/by/4.0/).

1. Introduction

Geomorphological mapping is based on the study, interpretation, and analysis of the evolution of the features of a territory [1,2]. Nowadays, the description and analysis of the earth's surface represents a product of high scientific value. These maps are able to provide a preliminary investigation of surficial processes and landforms, natural hazards, and

landscape evolution [3–6]. These products depict the morphographic and morphogenetic features of the surface, interpreting their origin according to past and present geomorphic processes that generated and modified them, and identifying their chronological sequence.

Geomorphological maps provide essential information for various scientific disciplines, e.g., hydrology, engineering, and ecology [7–9]. They represent an effective tool, usable in land management, geohazard assessment, and territorial zonation, which are essential elements for risk management and mitigation operations [3]. Effectual land use planning and risk management need a comprehensive investigation of both spatial and temporal distribution of geohazards as well as a proper geomorphological mapping of processes, landforms, and deposits. Traditional geomorphological maps are static products, mainly based on subjective descriptive approaches, which are time-consuming and struggle to represent the complexity of a landscape at various scales and its evolution over time [10]. These severely limit their use in risk management and mitigation, due to their insufficient capacity for providing a proper representation of the geo-hydrological phenomena of a territory.

A combined use of multi-source and multi-temporal data can represent an effective way to spatially and temporally describe destructive processes, such as active ground deformation phenomena or erosional and flood features, providing a partially quantitative description of landforms [11–13]. However, the management of data derived from different sources can pose a challenge in ensuring a cartographic product that follows standardized canons and rules and is simultaneously able to provide highly detailed information that can be useful in land preservation and management actions and suitable for adaptive strategies, actions, and decisions making.

Due to its predominantly hilly and mountainous territory, Italy is notoriously one of the most highly fragile of the European countries [14–16]. The entire national territory is widely exposed to geo-hydrological hazards, mainly represented by landslides, of various sizes and types, from local rapid slides to large slow-moving phenomena and various erosion processes, which play an important role in the short- and long-term landscape evolution and cause significant damage and economic losses as well as claiming human victims [17]. Geo-hydrological risk management and mitigation requires a concerted approach between administrative bodies at different levels, from local to national, often with the support of the scientific community, in order to provide effective, homogeneous, and standardized operational tools. In this context, the need for geomorphologically applicative mapping based on international standards able to guarantee a proper interchange and interoperability of geographical data has become necessary for territorial institutions. This has led to the creation of cartographic products structured with a hierarchical organization of the recognized features and easily manageable in a GIS environment [10,18].

In recent years, research in geomorphological mapping has shown progressive growth, leveraging remote sensing and GIS technologies, able to combine traditional on-field approach with modern techniques [19–21]. The increasing availability of digital terrain models (DTMs) planned by national and regional authorities has led to the generation of freely downloadable medium- to high-resolution data, mainly derived from Light Detection and Ranging (LiDAR) acquisition at regional scale [22–24], and also detected by LiDAR mounted on an iPhone [25]. Besides the LiDAR technique, digital photogrammetry and unmanned aerial vehicle (UAV) applications provide a wide variety of low-cost digital elevation models (DEMs) that can offer a very high resolution of data [26–28]. Such wealth of data represents a key element in landform recognition via remote landscape characterization, through the automatic extraction and classification of landforms employing submeter resolution DEMs with relatively high accuracy [29,30]. The availability of DEMs having different resolutions allows for an optimal geomorphometric description of landforms of

various sizes as well as of a hierarchy of the landforms [31]. The recognition of landforms can be performed by primarily leveraging the main land surface parameters, i.e., DTM derivative products such as slope, shaded relief, profile, and plan curvature. The combination and overlapping of these land surface parameters allow the manual identification and mapping of geomorphological features by visualization techniques [32,33]. Moreover, automated and semi-automated landform classification, based on terrain analysis via DTMs, has been developed [34–36] and is currently available in the form of GIS tools [37–39]. These landform classifications are based on diverse geomorphometric parameters and their combination to derive geomorphic units [40] or specific landforms (e.g., channel morphology [41], landslide crown and bank erosion [42], and gully [43]); these are often compared with each other [44,45]).

Through these unsupervised or semi-automatic procedures, a classification of landforms is provided, overcoming the time-consuming procedure of traditional on-field geomorphological mapping. Although these approaches ensure a preliminary remote spatial pattern of landforms, their accuracy is scale-dependent (preferably being at the mesoscale). Moreover, most geomorphological algorithms are derived from DEMs by neighborhood analysis (proximity analysis), based on the assumption that landform types are discernable via comparison to the corresponding neighboring elements. There is then a dependence on correctly setting the search parameters [46]. Despite the cost-effective and time-efficient features of automated landform classification, due to the described limits in the literature, such methodologies are often integrated with traditional terrain surveys [47,48]. Moreover, the use of these approaches does not provide any temporal information or information about the origin of the features [49], requiring further investigations. The need to modernize the generation of geomorphological maps represents an issue to be addressed, mainly in terms of the creation of scalable geomorphological maps and increasing their ability to spatially and temporally characterize the landforms and processes acting on diverse physiographic areas. Accordingly, to achieve a more time-effective geomorphological mapping compared to traditional maps, a methodology based on multi-source data, able to spatially and temporally recognize landforms and their morphogenesis via remote sensing applications, may represent an effective system to be deepened and investigated.

The aim of this work is to increase the understanding of landscape from a morphometric and morphogenetic point of view, through the implementation of new approaches for the description of geomorphological processes and representation of landforms. A methodology based on multi-source data and multi-sensor application was implemented for the spatial and temporal recognition of landforms and processes. This procedure was applied and tested in an Apennine basin located in Val d'Orcia, Tuscany Region. Leveraging regional-derived LiDAR data, and collecting and digitizing a time series of historical orthoimages, a slope-scale investigation and extraction of landforms was planned. By executing a UAV survey on the most active sectors, 3D data computing was used to provide a high-resolution digital terrain model (DTM) and orthoimage, digitalized to obtain detailed geomorphological mapping at local scale.

The proposed approach guarantees a multi-scale and multi-temporal cartographic model that is digitally manageable, offers a full-coverage representation of landforms and processes acting over time, and is representable via scalable geomorphological maps, providing a useful tool for decision-makers in every action and decision concerning the territory.

2. Materials and Methods

To design new paradigms for geomorphological mapping that can overcome the traditional cartographic approaches, thus improving the operational readiness of geomorphological maps, especially for risk management and mitigation, a multi-source methodology able to integrate the morphometric and morphological analysis was developed. Integrating multi-source remote-sensing data, we operated to capture the main landforms of a territory in a scalable mode and assess the landscape morphogenesis via a fully remote approach. Operating in a GIS environment, the proposed approach ensures both spatial and temporal investigations, allowing the rapid characterization of the morphologic evolution of a territory and scalable, full-coverage geomorphological mapping. Figure 1 shows the scheme of the implemented methodology, here applied in a pilot area, i.e., Fosso della Piaggia catchment, Tuscany Region.

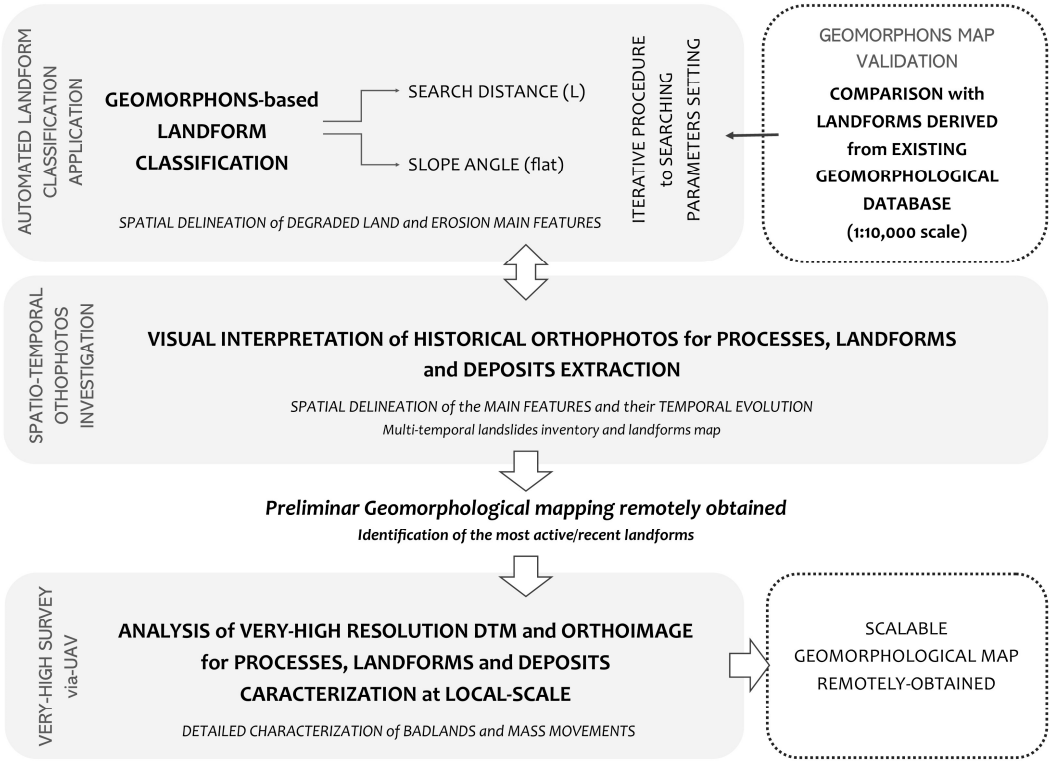


Figure 1. Conceptual scheme of the implemented methodology.

2.1. Pilot Testing Area

The Fosso della Piaggia basin corresponds to a small catchment (about 2,100,000 m^2) located in the Radicofani municipality, Siena Province, Tuscany Region, Italy (Figure 2), having an extent of 11.708°E, 42.944°N ÷ 11.734°E, 42.956°N. This area is located in the renowned Val d'Orcia territory, a smooth, hilly landscape in the southern portion of Tuscany. Morphodynamically, runoff-associated landforms coexisting with gravitational processes dominate this territory, primarily occurring in the Plio-Pleistocene marine clays of the Apennine piedmont [22,26,50]. Surface water runoff processes promote the formation of badlands, i.e., 'calanchi', typical landforms very widespread in the Apennines. The identified testing area represents an end-member of the southern Tuscan Apennine territory, consisting of a gently sloping catchment primarily affected by widespread calanchi areas and large ancient mass movement.

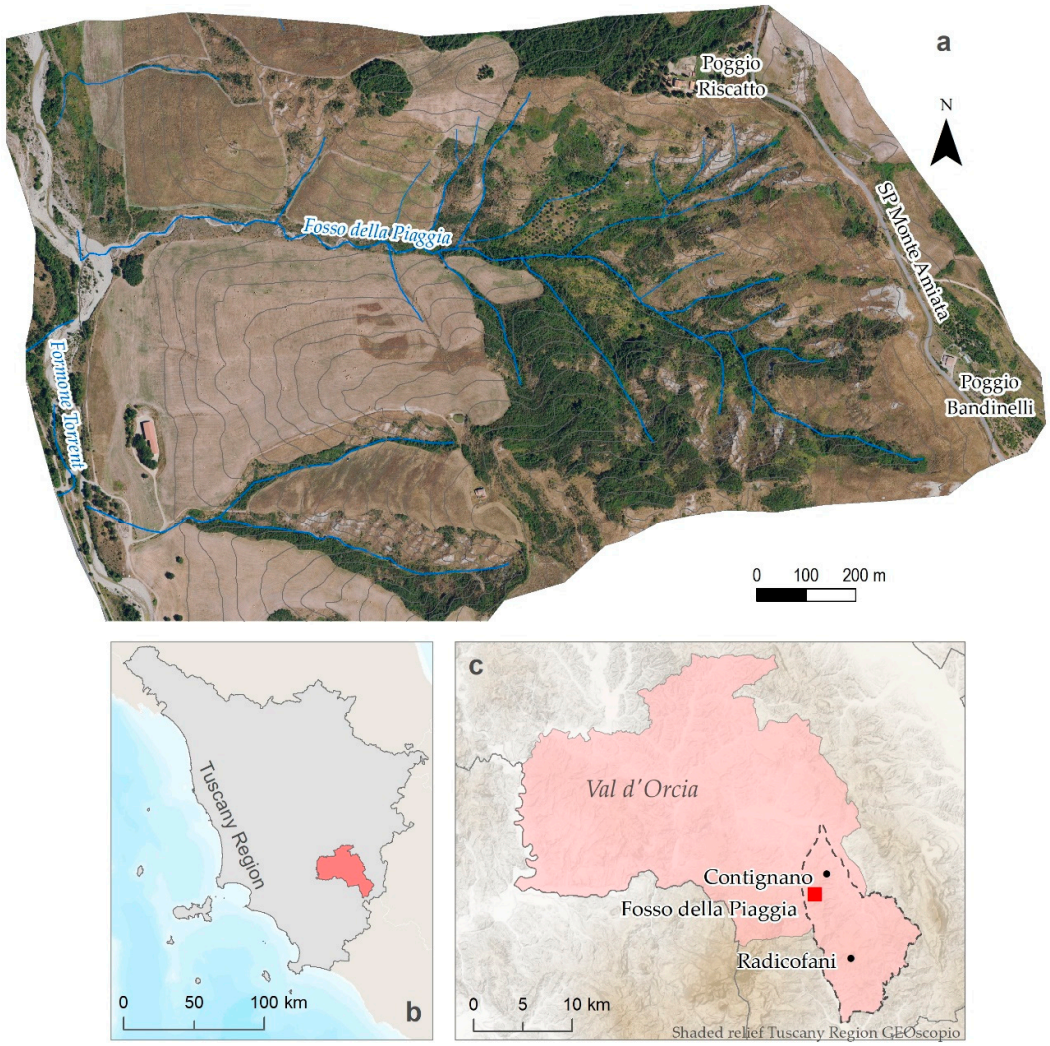


Figure 2. (**a**) Location of the testing area of Fosso della Piaggia basin, Radicofani municipality, Tuscany Region, (**b**) sited in the renowned Val d'Orcia hilly territory (**c**), southeastern Tuscany.

Morphologically, the regional geomorphological database, supplied by the Department of Urban Planning and Housing Policy, Tuscany Region, provides a 1:10,000 scale overview of the morphological setting of the area of interest (Figure 3), and it is available online in the regional web portal [51]. In the "Geomorphological DB", geomorphological entities are organized into "strata" classified according to "genesis" and "state of activity" of the landform criteria. The morphogenesis of landforms, processes, and deposits identifies the origin of the forms, differentiated by using different colors referring to the diverse endogenous and exogenous processes (e.g., green for surficial water runoff and erosion). The morpho-evolution of the landforms is attributed on the basis of their state of activity, if determinable, distinguishing between active/in evolution, quiescent, and stabilized landforms. Extended quiescent rotational slides can be recognized in the selected area (Figure 3), set in the marine clays, locally alternated to gravelly levels. Large mass movements, mainly represented by roto-translational slides or earth/mudflows, are distributed in the upper-medium portion of the basin, interposed between badlands landforms and visibly re-shaped by surface water runoff processes, e.g., gully, erosive scarp. The calanchi correspond to small catchments characterized by very steep slopes (35–50°), dense and hierarchized drainage networks that promote a dense alternation of narrow V-shaped valleys with typical knife-edge erosional features, often the source of localized surficial slides. The most extensive badland landforms have developed in the upper portion of the

basin, on both south- and north-facing slopes of the catchment, characterized by very steep slopes and small V-shaped valleys, less vegetated on the south-facing slope in comparison with the northern one. The most important mass movement has almost totally affected the upper part of the basin, from Fosso della Piaggia river up to the main road (SP Monte Amiata); this ancient slide has been visibly reshaped and progressively dismantled by erosional processes, such as erosional scarps or rills and gullies erosion. Other large mass movement has occurred along the main hydrographic network, visibly reshaped by human intervention (e.g., olive groves). The downstream portion of the basin is characterized by a strong anthropic footprint, with extensive arable lands that have reshaped and obliterated the natural landforms of the slopes.

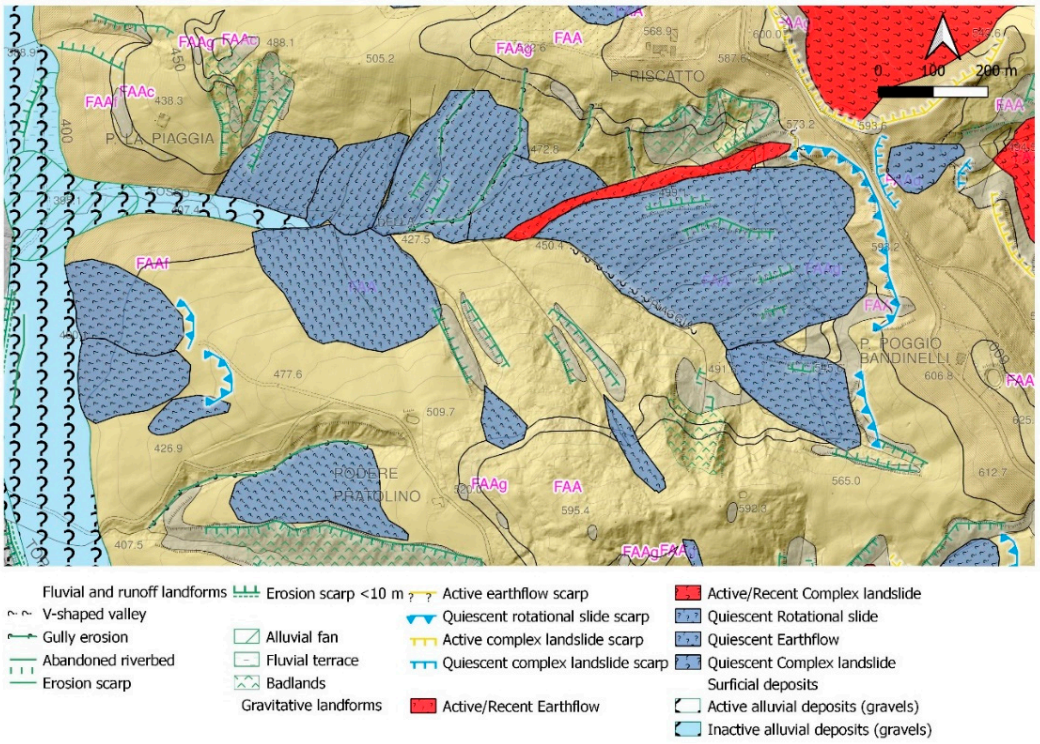


Figure 3. Extract of the geomorphological map derived from data in the Geomorphological DB of Tuscany Region corresponding to the testing area, Fosso della Piaggia basin; the main geological unit outcropping in this territory corresponds to Pliocene marine deposits (clay and silty clay (FFA), olistostromes of Ligurian material (FAAc); clay with Ligurian limestones (FAAf); resedimented conglomerates (FAAg)).

2.2. Automated Landform Classification Application

Thanks to the availability of pre-existing regional DTMs, a 1m resolution LiDAR DTM of 2012 available from the regional portal, i.e., the Tuscany web portal [51], an examination of the morphometry and delineation of surface topography was performed using automatic landform classification (ALC), i.e., the Geomorphons approach [52]. ALC allows the detection of the main landforms via DTM segmentation through an automatic or unsupervised geomorphic classification of elementary land units, adhering to imposed geometric constraints. Starting from a simple DTM, ALC facilitates a general overview of the spatial distribution of landforms, primarily defining and reconstructing the articulated relationships of the diverse landforms with respect to the landscape evolution. Operating in the open-license GIS platform SAGA GIS [53], the Geomorphons approach was implemented, performing an iterative procedure aimed at establishing the most suitable attributable search parameters. Several principal DTM-derivative products, e.g., slope, aspect, contour,

profile, and tangential curvature, were also derived to obtain an overall analysis of the topography, as well as to obtain input data essential for the application of this ALC.

2.2.1. Geomorphons-Based Classification

The Geomorphons-based landform classification was proposed by [52], corresponding to a pattern recognition technique using a local ternary pattern. The topographic variability is assessed by computing the increase, decrease, or unchanged elevation of a grid DTM cell. This approach [35] considers the line-of-sight principle to evaluate the 8 neighboring grid cells, labelled either 0 if the grey level of a neighbor is smaller than the grey level of the central cell, or 1 otherwise. By this approach the ternary pattern is determined, considering not only the elevation parameter but also the zenith and nadir angles in the lookup distance using the line-of-sight principle. The landform classification is obtained by delineating the Local Terrain Patterns (LPTs) corresponding to the principal base elements that constitute the most common recognizable Geomorphons: flat, peak, ridge, shoulder, spur, slope, hollow, footslope, valley, and pit.

In our methodology, for the Geomorphons application, an iterative procedure was carried out for testing and comparing the setting distances for different parameters. A number of tests were first performed to optimize the parameters of the Geomorphons tool of SAGA GIS, which represented the categories of terrain forms from a digital elevation model using a machine vision approach. The algorithm is based on several parameters: the "search distance" (L) is the distance away from the target cell that defines the radius of the area that will be used to identify the Geomorphons pattern, and the "flat terrain angle threshold" (flat) corresponds to the angle threshold below which the target cell will be classified as flat. Due to the medium-to-high resolution of the input DTM used, the flat terrain angle threshold was kept to the default value (1 degree), and a testing phase of "search distance" was carried out to define values that would better match the type and size of the landforms to be classified. The tested values for the L parameter were 5 m, 10 m, 25 m, 50 m, and 100 m. Comparing the intermediate outputs with the shaded relief map (Figure 4), the lower L values show a rather noisy representation (L = 5 m), progressively improved by setting higher L values (L = 10 m, 25 m).

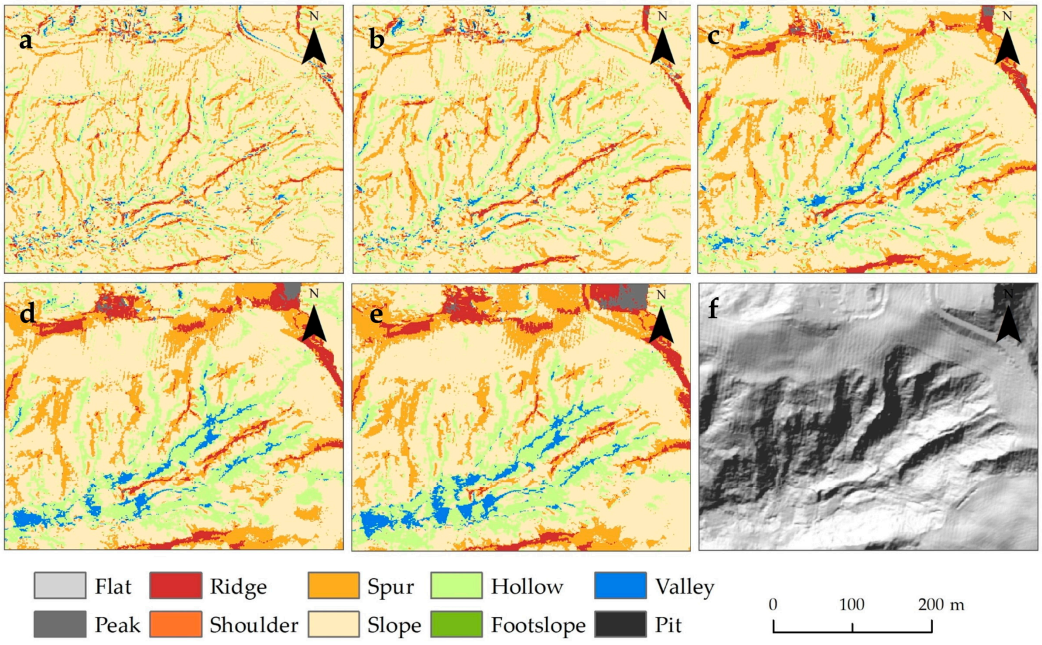


Figure 4. Comparison of the Geomorphons intermediate results obtained by varying the L parameter: (**a**) 5 m, (**b**) 10 m, (**c**) 25 m, (**d**) 50 m, and (**e**) 100 m, with (**f**) shaded relief map of the investigated area.

High L values (L = 50 m, 100 m) returned a too coarse representation of the territory, misclassifying the topographic position of both the ridge/spur and stream Geomorphons. A search distance of 25 m was finally imposed.

2.2.2. Geomorphons Map Validation

In order to validate the preliminary morphological representation obtained via the application of Geomorphons, a comparison with the available Geomorphological DB of the Tuscany Region was carried out. The vector data were derived from this institutional database.

We converted the ALC raster in a vector format and then, iteratively, selected the linear features from the Geomorphological DB intersecting with the Geomorphons subset, thus obtaining a series of comparison subsets. Therefore, a quantification of the frequency of the corresponding geomorphological classes was accomplished. The procedure was also repeated on the hydrographical network. All the processing was fulfilled in GIS [54] and R programming [55] open source environments.

2.3. Spatio-Temporal Orthophoto Investigation

Thanks to the increasing availability of national and regional orthophotos, an examination of the historical images was carried out to obtain a spatial and temporal delineation of the morpho-evolution of the area of interest. A collection was made of historical orthophotos derived from regional and national institutional sources, i.e., the Tuscany regional web portal [51] and the National Cartographic Portal [56], and partly from the Google Earth service. The orthophotos were made available from diverse sources and with different formats, as summarized in Table 1, covering an observation period of about 67 years.

Table 1. Summary of the orthophotos collected from national and regional sources for the testing area.

Source	Operator	Date	Scale	Format
Regional Web Portal	RT volo Rossi Brescia	1954	1:10,000	.tif
	IGM-RT volo Gruppo Aereo Italiano	1978	1:10,000	.tif
	AGEA	2002	1:10,000	wms
	BLOM-CGR volo BLOM CGR	2007	1:10,000	wms
	AGEA volo Rossi Brescia	2010	1:10,000	wms
National Cartographic Portal	RT volo CGR Parma	1988	1:10,000	wms
	AGEA volo CGR Parma	1996	1:10,000	wms
	BLOM CGR S.P.A	2000		wms
	BLOM CGR S.P.A	2006		wms
	AGEA	2012		wms
Google Earth	n.a.	2001		kml
	n.a.	2013		kml
	n.a.	2016		kml
	n.a.	2017		kml
	n.a.	2019		kml
	n.a.	2021		kml

Operating in a GIS environment, the geometrically identifiable "entities" (i.e., polygons, polylines, points) are identified, in order to assess geomorphological evolution of the territory investigated, through the mapping of landforms and deposits over time. A multi-temporal investigation of the main landforms and processes was carried out, through a photointerpretation of the collected orthophotos. Considering a progressive set of images, we attributed the relative age of the identified phenomena, over the observation period of about 67 years. A landslide hierarchy was discriminated, distinguishing between the oldest landslides—i.e., ancient landslides visibly dismantled and reshaped, so that part of their original border has to be partially inferred, but it is still connected to the present-day

local base level [57,58]—and the observable fresh or recent landslides identifiable between two subsequent images. Following these criteria, the landslides and the main erosion features were classified and mapped according to their estimated relative age. The landslides mapped were classified according to [59,60]; all the features and landforms were also classified following the "Quaderno 13" [61] guideline recognized at the national level.

The combined analysis of historical orthophoto investigation with ALC application allows a preliminary geomorphological mapping, at basin scale, devoted to identifying the portions of territory affected by the most active and recurrent processes, over which a local scale characterization will be necessary.

2.4. Unmanned Aerial Vehicle (UAV) Survey

An ad hoc unmanned aerial vehicle (UAV) survey was carried out on 12–14 May 2024, using a DJI Phantom-4 equipped with an RGB camera (SZ DJI Technology Co., Ltd., Shenzhen, China). The flight was carried out at an altitude of 45 m, due to flight regulation in the area, and materialized 10 reference targets. Ground Control Points (GCPs) were measured with a GNSS receiver adopting an RTK-VRS technique, for proper georeferencing of the entire flight. The mean errors of the GCPs in the three coordinate directions are reported in Table 2.

Table 2. Summary of the GCPs' mean errors in the three coordinate directions of the RPAS flight carried out in the Fosso della Piaggia basin, Val d'Orcia.

	Error X [m]	**Error Y [m]**	**Error Z [m]**
Mean (m)	−0.019561	−0.006316	−0.063786
Sigma (m)	0.076436	0.055568	0.185325
RMS Error (m)	0.078900	0.055926	0.195995

The flight produced 2170 images acquired with an overlap of 80% and a sidelap of 70%, post-processed by PIX4D mapper (version 4.9.0) software, generating a point cloud consisting of more than 220 million points (3D Densified Points amounting to 226,550,601 with an average density of 367.77 per m^3). A very-high-resolution DEM and orthoimage, with an average Ground Sampling Distance (GSD) of 2.59 cm/pixel, were obtained.

The UAV flight covered the upstream portion of the Fosso della Piaggia basin, recognized via ALC and historical photos from previous examinations as the most active sector of the investigated area. The very-high-resolution UAV-derived products allow a detailed geomorphological mapping, which is useful to describe those sectors mainly characterized by runoff-associated landforms coexisting with gravitational ones and for recognizing portions mainly subject to rapid change and high erodibility.

3. Results

By applying the proposed approach, a full coverage is obtainable of the topographic surface, organized in two main levels, facilitating a spatial and temporal recognition of landforms and processes. A slope-scale geomorphological characterization is gained via (i) an automated spatial delineation of degraded land and erosion features by LiDAR data exploitation and (ii) a spatial description of the main features and their temporal evolution by the interpretation of historical orthophotos. This level allows a remote characterization of the area of interest, identifying the most active and/or recent, potentially hazardous, landforms. The focused analysis of these sectors via a UAV survey allows (iii) a local scale geomorphological mapping using very-high-resolution derivative products, for a second level of deepening of the phenomena and processes acting in the investigated area.

3.1. Spatial Delineation of Degraded Land and Erosion Features

A preliminary examination was made of the morphometry and delineation of surface topography, with an investigation and extraction of the main degraded sectors and erosion features, leveraging pre-existing metric DTMs analyzed using Geomorphons-based ALC. Figure 5 shows the map obtained via Geomorphons application in the Fosso della Piaggia area. The spatial outlining of the main features is obtained, delineating the patterns that characterize the main gravitative and erosional features of the testing area. The result of the Geomorphons application shows a prevalent dual pattern: an upstream portion with a prevalence of dense alternation of ridge areas and sectors, with a highly irregular pattern, and a downstream portion that is less irregular, with a prevalence of slope areas (31%) with local spur and hollow zones (10% each). A small percentage of the study area is then represented by ridge (3%) and valley (2%). Other classes cover a negligible surface of the site. The reliability of the method was assured by validation, obtained by comparing the features with the Geomorphological DB; the best performance was obtained by a comparison of the valley Geomorphons type with the hydrographic network, with a 93.75% correspondence. The linear features compared with ridge scored 86.67%, and there was complete correspondence with the landslide outline feature class. Arable land management and maintenance have reshaped the valley flanks in this downstream portion of the basin, excluding a sector defined by two long spurs bounded with prevalent active surface runoff processes. By contrast, the upper portion of the basin shows a highly irregular pattern, in which it is possible to distinguish the main processes and forms acting in this territory.

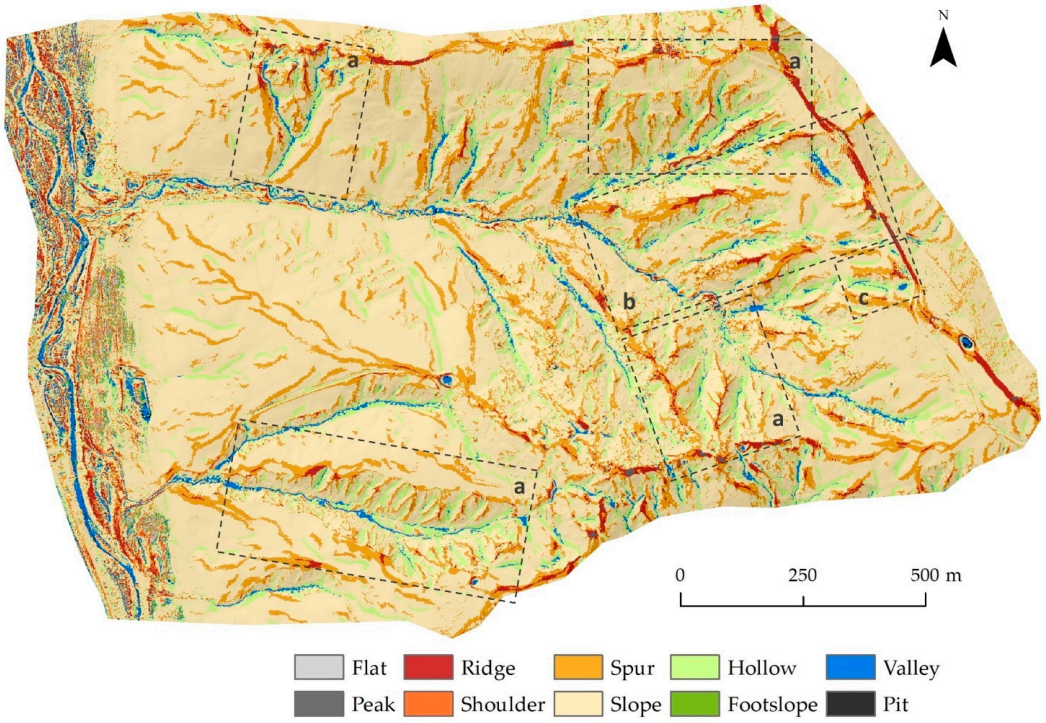


Figure 5. Geomorphons map at the scale 1:10,000 of the Fosso della Piaggia basin testing area; the subsectors depicted highlight the end-members of the Geomorphons landscape representation corresponding to the main processes and landforms of the investigated territory: **a**, calanchi area; **b**, ancient large mass movement; **c**, distinct form with spur/ridge values alternating with a hollow area.

The subsectors depicted in Figure 5 indicate the main patterns recognized via the Geomorphons application, describing the principal processes and landforms. Subsector "a" depicts a terrain dominated by a dense alternation of narrow valleys delimited by mainly north–south oriented extended ridges and spurs. These subsectors can be mainly

associated with the calanchi portions of the testing area, which upstream are bounded by main erosional scarps (ridge values), which locally demarcate the watershed of the catchment, corresponding to the main roads. Subsector "b" identifies a zone featuring a more complicated morphology, evidence of a very long and complex evolutionary history. In this subsector, we observed a ridge area that delineates a main scarp in the upper part of the basin, close to the road network, delimiting the large ancient mass movement affecting this area. In this portion, the terrain results were characterized by a series of extended ridges and/or spurs parallel to the slope, alternated with hollow/valley landforms, evidence of active runoff processes able to dismantle and remodel the landslide deposits. Moreover, a local counter-slope sector can be recognized in the upper portion of the slope, delineated by the alternation of areal portions respectively with valley and ridge classes. This conformation could result from the rotational kinematics of the large mass movement affecting the slope.

Between the northeast calanchi area and the ancient large mass movement affecting the upstream portion of the basin, a noticeable east-northeast–west-southwest oriented elongated channel can be recognized, highlighted by an extended linearly hollow area, with valley values indicating high erosive power.

A particular case is the area defined by the subsector "c", where an areal portion, with spur/ridge values alternating with a hollow area, can be observed along the slope close to the SP Monte Amiata that corresponds to Poggio Bandinelli. At the basin scale, this landform is difficult to interpret; the Geomorphons map surely provides initial evidence by highlighting a distinct form of the territory, necessitating a local-scale investigation.

3.2. Spatial Delineation of the Main Features and Their Temporal Evolution

The historical orthophoto investigation allowed us to extract the main landforms, processes, and deposits of the investigated territory over a 67-year time span. The delineated landforms, together with Geomorphons-based landform delineation, revealed a typical Apennine landscape characterized by active erosive and gravitative processes mainly occurring in clay soil: widespread calanchi areas, mainly distributed in the upper portion of the basin, are often associated with local earthflows and mudflows, and giant ancient rotational slides have been deeply remodeled by the erosive action of surface water runoff and by gravitative phenomena. Figure 6 shows the multi-temporal landforms and landslides inventory obtained at the basin scale via geomorphological photointerpretation.

The map highlights numerous landslide events that occurred over the past decades, mainly corresponding to local earthflows and mudflows, and more extended rotational slides. Most of the localized earth- and mudflows occurred in the upper part of the basin, corresponding to the south-facing calanchi area, close to the Poggio Riscatto farm, and corresponding to the extended quiescent rotational slide deposit, close to the Provincial Road of the Monte Amiata. The overall framework delineated testifies to the rapid evolution of the badland landforms, mainly in the northeastern portion of the area, and a noticeable remodeling of the ancient mass movement by erosional and gravitative processes over time.

To be noted the large complex landslide that occurred in the period from 1978–1988, involved the deposit of the large mass movement extending from the SP Mt. Amiata and the Fosso della Piaggia river. This event started as a rotational slide and evolved into an earthflow. Precursor signs are recognizable in the 1978 image (Figure 7a), with the paroxysmal phase occurring in 1988 (Figure 7b), during which the landslide deposits interfered with the hydrographic network, partially modifying the watercourse trend. In 1996, slope adjustment due to earthmoving can be observed along the entire slope (Figure 7c), with a re-shaped landslide deposit clearly recognizable in the 2007 orthophotos (Figure 7d).

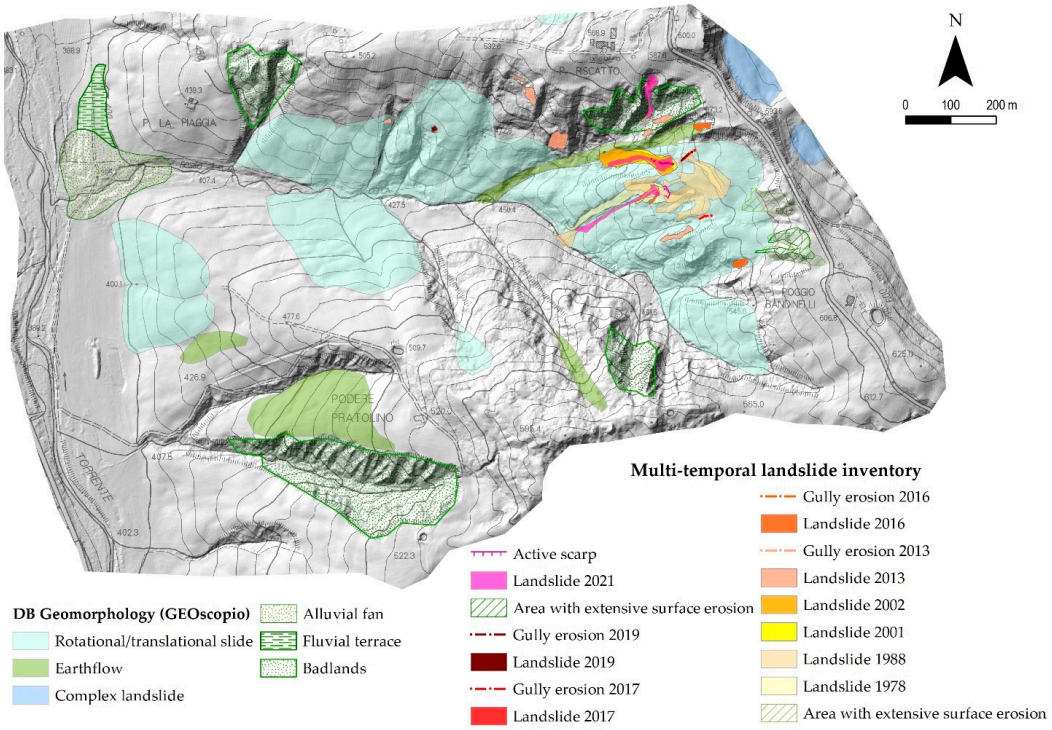


Figure 6. Multi-temporal erosion processes evolution and landslide inventory map obtained by investigation of historical orthophotos (observation period 1954–2021) of the Fosso della Piaggia basin, Contignano, Val d'Orcia.

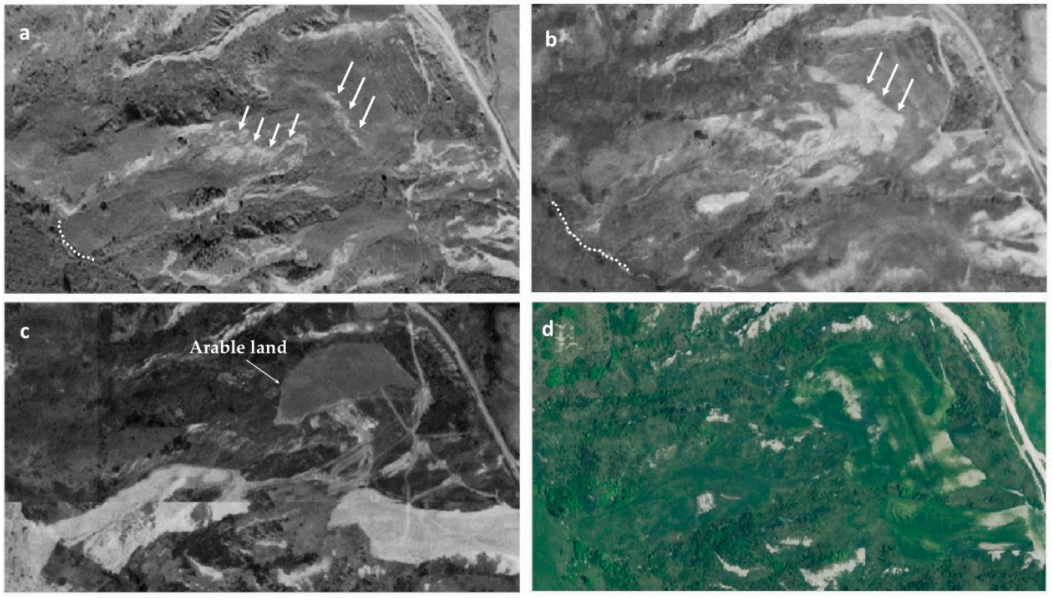


Figure 7. Visual comparison of the large complex landslide involving the deposits of the ancient rotational slide that affects the slope from the SP of Monte Amiata up to the Fosso della Piaggia river: (**a**) first evidence of reactivation of the middle portion of the ancient slide in 1978, with (**b**) paroxysmal phase in 1988, followed by (**c**) anthropic interventions along the slope in 1996, with an extended earthmoving in the downstream portion, still well-recognizable in (**d**) subsequent orthophoto of 2007. White arrows depict the active scarp while dotted line the landslide foot.

In the upper portion of the basin, besides the large ancient landslide close to the provincial road, the badland landforms characterize the entire sector. The south-facing calanchi areas show steep slope and narrow V-shaped valleys (Figure 8), with a general lack of vegetation and a recurrence of mudflow events (Figure 8g–i) higher than those on

north-facing areas, characterized by a more extensive shrub and herbaceous vegetation. Close to Poggio Riscatto farm, the calanchi evolution has progressively interfered with the arable lands upstream (Figure 8a–d), as noticeable from the 1996 orthophoto. Gully, interrill, and rill erosion have affected these landforms, favoring the neo-formation of other calanchi areas, as observed in the central portion of the upper part of the basin (Figure 9a–h), close to the Poggio Bandinelli farm.

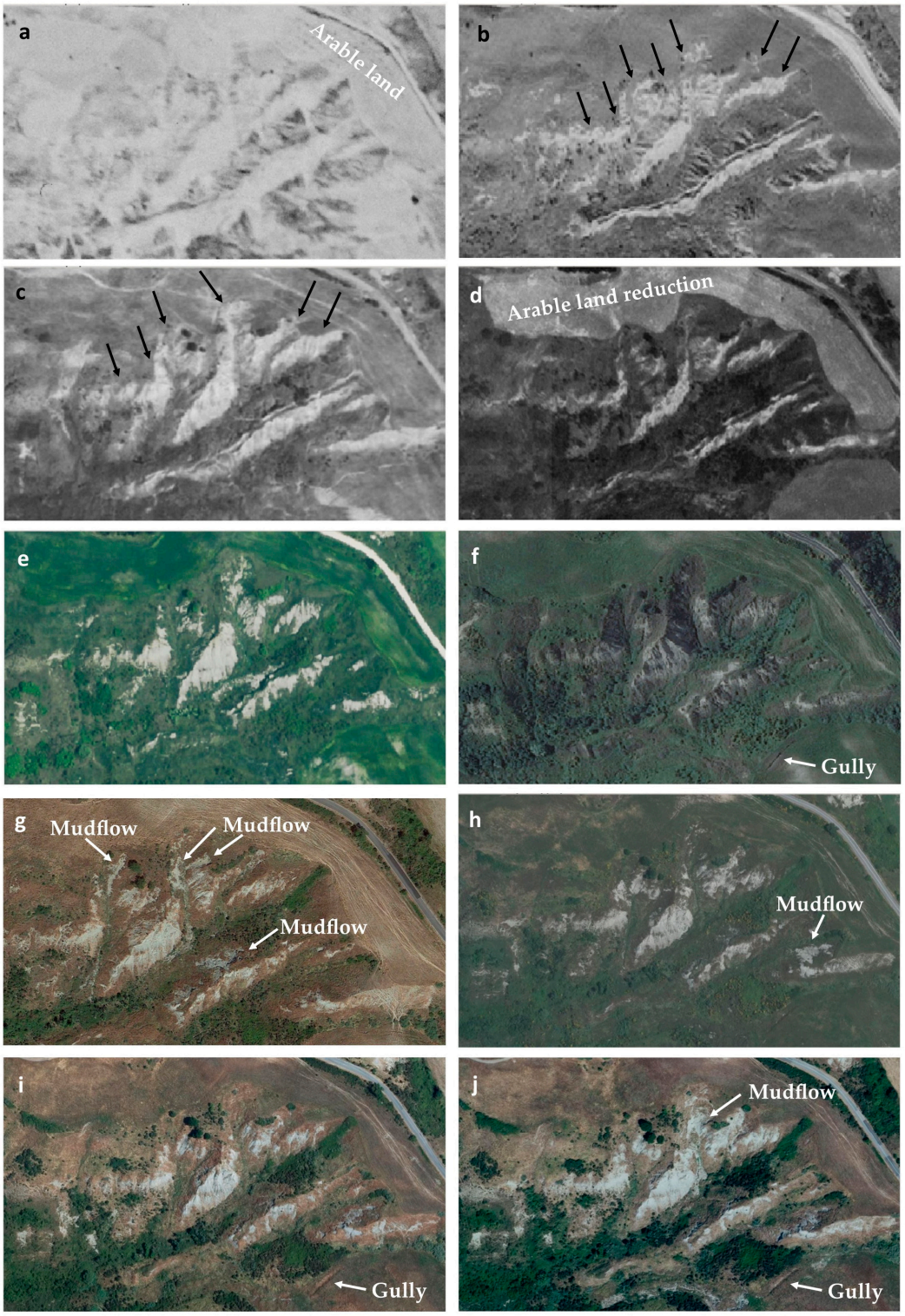


Figure 8. Visual comparison of the south-facing calanchi area, close to Poggio Riscatto farm, in the upper portion of the catchment, with a general retrogressive trend affecting the arable land upstream and associated to earthflow/mudflow events over time: (**a**) 1954, (**b**) 1978, (**c**) 1988, and (**d**) 1996 progressive

extension of calanchi area, with relevant reduction of the arable land in 1996, (**e**) 2007, (**f**) 2010, (**g**) 2013, (**h**) 2016, (**i**) 2019, and (**j**) 2021, with recurrent earth- and mudflows localized in the narrow valleys of the calanchi area and erosion of gullies. Black arrows depict the active scarps.

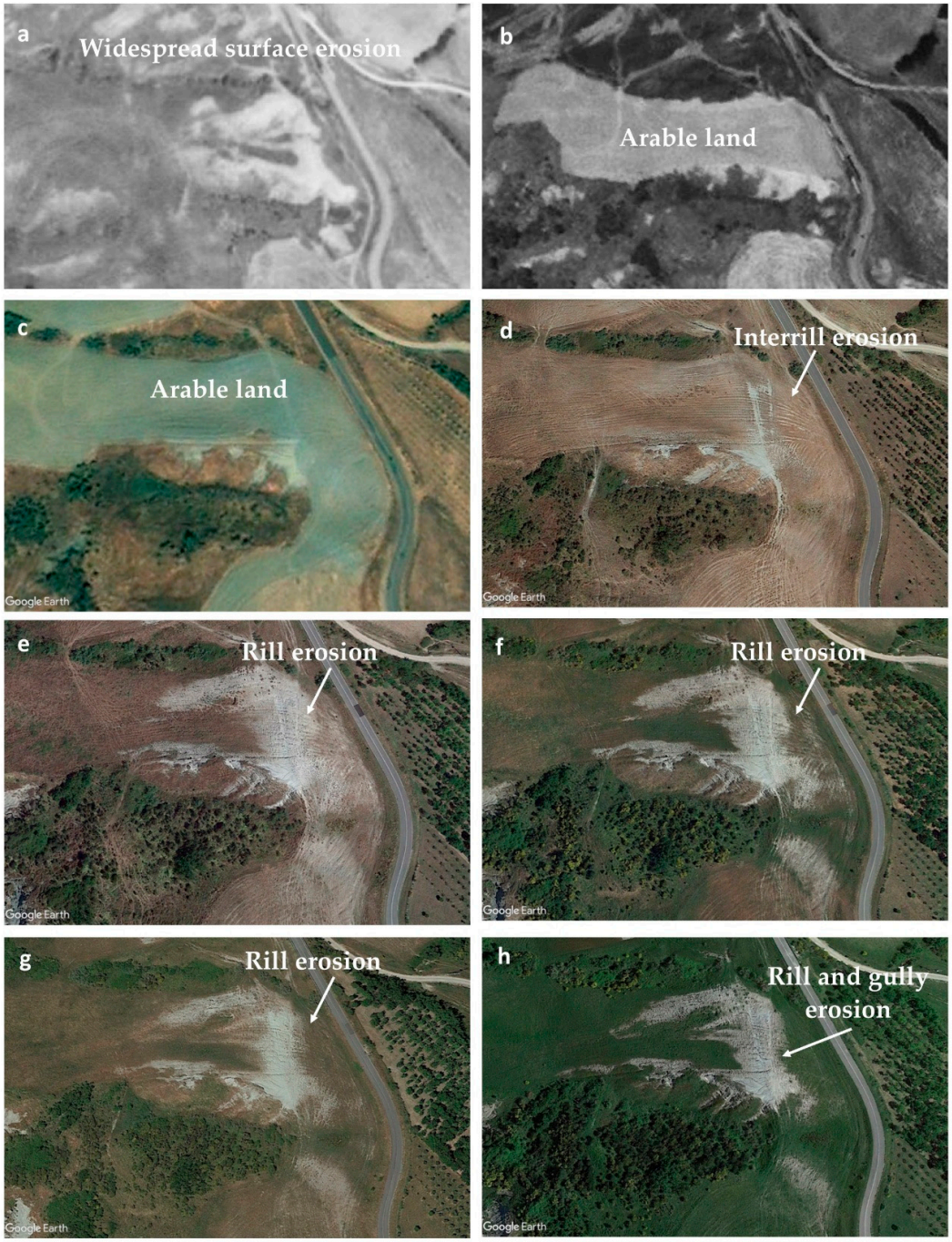


Figure 9. Visual comparison of the progressive surface erosional processes affecting the arable land close to the Provincial Road of the Monte Amiata: (**a**) 1988–1989 orthophotos with clearly recognizable areas characterized by widespread surface erosion; (**b**) 1994–1998 orthophotos, showing that the previous area has been completely reshaped by human intervention for agricultural purposes; (**c**) 2001 orthophoto, in which arable land shows previous effects of runoff, followed by progressively (**d**) interrill erosion in 2013, rill erosion in (**e**) 2016 (**f**), 2017, and (**g**) 2019 orthophotos, and rill and gully erosion in (**h**) 2021, favoring the formation of new badland landforms.

3.3. Local Scale Geomorphological Mapping with Very-High-Resolution UAV-Derivative Products

Based on the previous intermediate results, the areas widely exposed to slope instabilities and erosion processes were recognized and further investigated via UAV survey. Lever-

aging very-high-resolution RGB orthoimage, combined with the main DTM-derivative products (e.g., shaded relief, slope, aspect, contour lines), all the visible landforms and processes visible on the 12–14 May 2024 flight were extracted and mapped to generate a geomorphological map at local scale.

In the south-facing calanchi area (Figure 10), close to the Poggio Riscatto farm, marked erosional scarps bordering on the arable lands are identifiable. Along these scarps, numerous "fresh" local surficial landslides are recognizable, mainly represented by mud- and earthflows (Subsectors "a" and "b"). Local shallow landslides affect the grassland cover, mainly distributed in correspondence with the barely grassed shoulders of the narrow valleys forming the calanchi area. To be noted is an extensive mudflow (Subsector "a" in Figure 10), visibly affecting the main scarp and eroding the arable land less than 100 m from the Provincial Road, which testifies to the general retrogressive trend of the badlands.

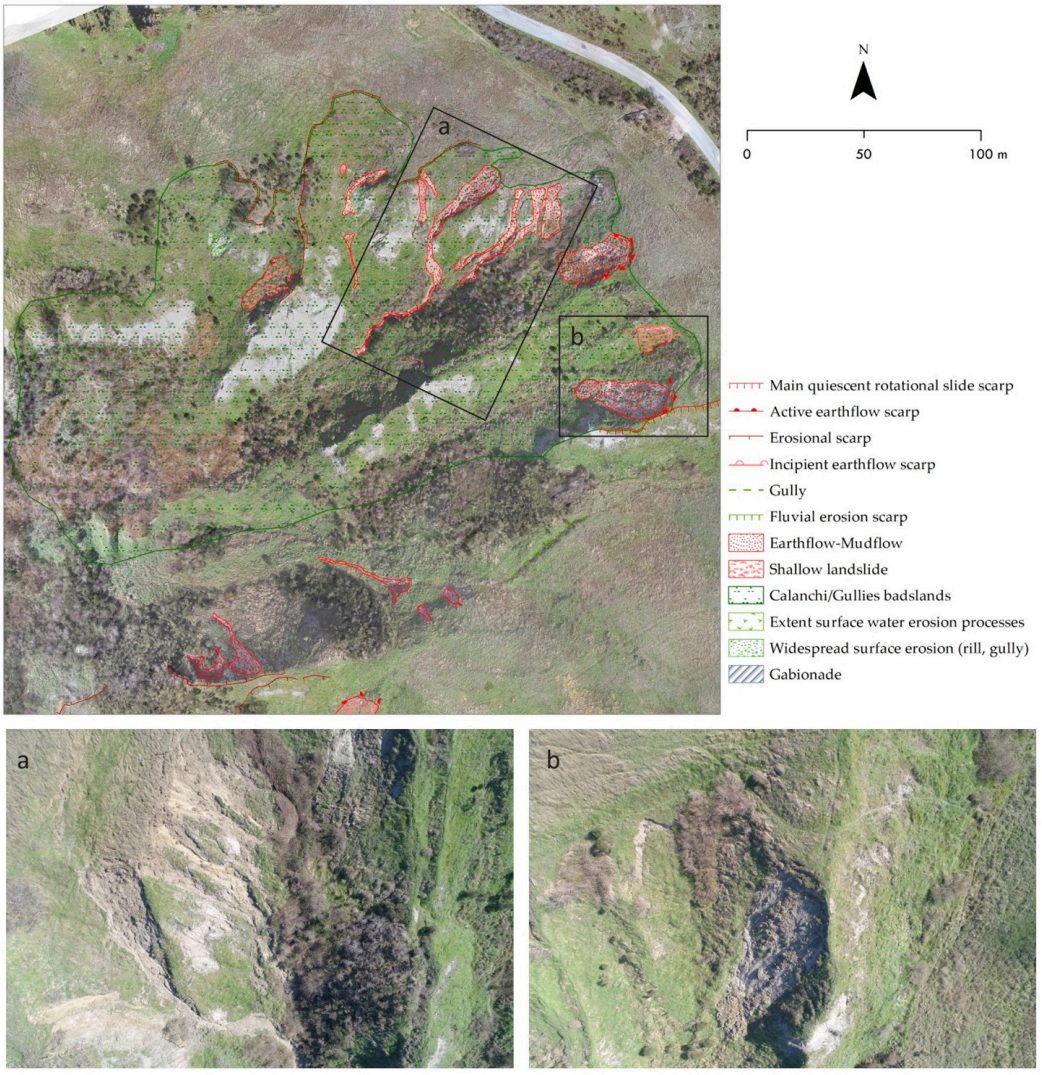


Figure 10. Local-scale geomorphological mapping derived from the visual inspection of the May 2024 UAV orthoimage, corresponding to the south-facing calanchi area, close to Poggio Riscatto farm, with some detail of (**a**) recent and "fresh" mud- and earthflows and (**b**) shallow landslides clearly identifiable.

Also, in the north-facing calanchi area, despite the more developed vegetation mostly represented by shrubs and trees, widespread mud- and earthflows can be recognized along the dense drainage network of the badlands (Figure 11). In the middle of the badland areas, the ancient rotational slide deposits, which extend from the main road to the Rio Piaggia,

show continuous remodeling by local surficial slope instabilities as well as by runoff erosive processes. Corresponding to the main scarp, partially stabilized with gabionades, local small shallow landslides are still recognizable, along with the erosional scarps in the middle and downstream portion. A persistent gully incision, extending for about 45 m, can be observed in grassland in the upstream portion of an exposed channel in the northwest, the site of recurrent mud- and earthflow events, as periodically recognized in multi-temporal analysis.

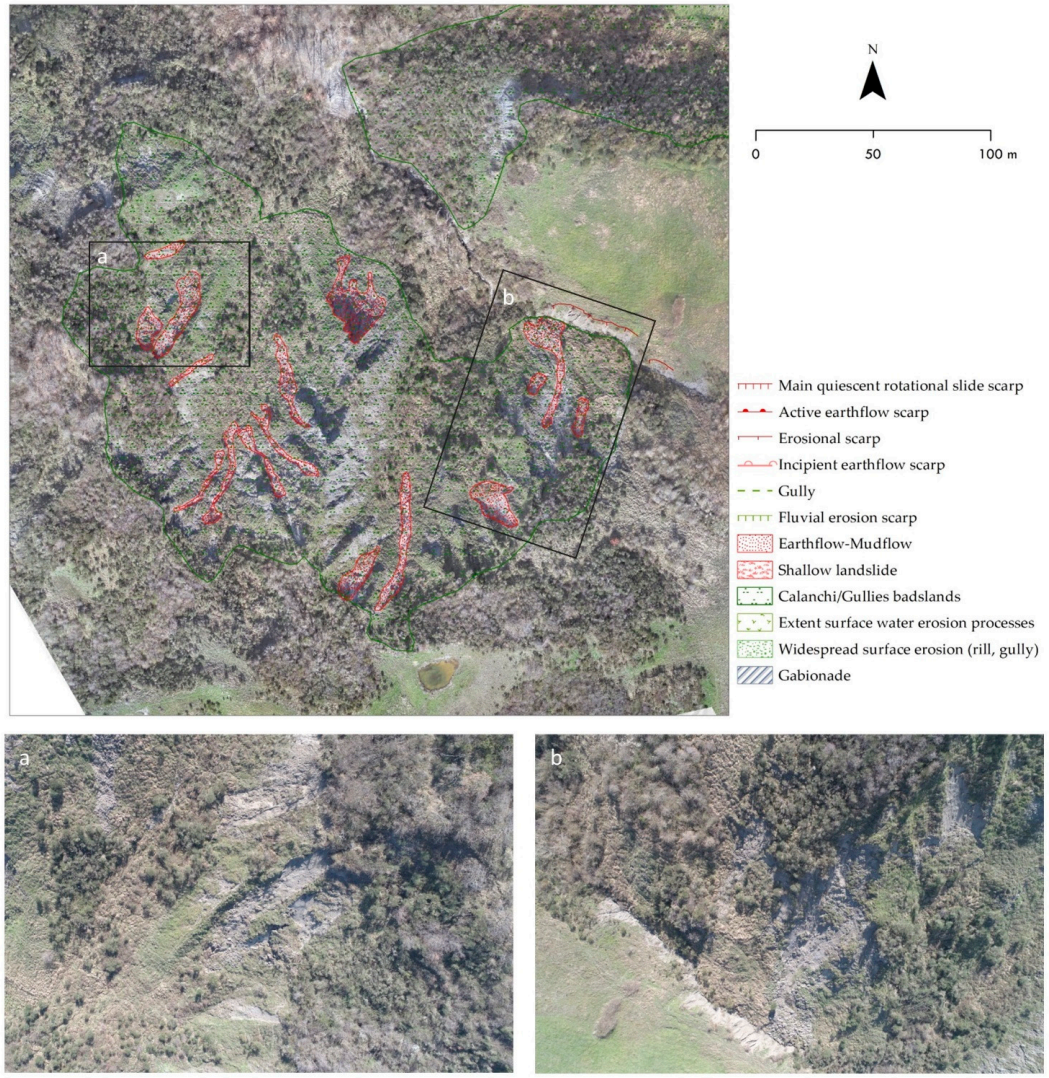


Figure 11. Local-scale geomorphological mapping derived from the visual inspection of the May 2024 UAV orthoimage, corresponding to the north-facing calanchi area, with (**a**,**b**) some detail of recent mud- and earthflows clearly identifiable.

In addition to gravitative processes, several landforms related to runoff water effects are frequently found throughout the area. Evidence of rill and gully incisions and tunnel erosion is widespread both in the calanchi areas and corresponding to the deposits of the ancient landslides that affect the entire upstream portion of the basin, often affecting the arable lands. It is important to note the persistence of the badlands in neo-formation (Figure 12), already identified in the visual interpretation of the historical orthophotos, and highlighted via ALC by spur/ridge values alternating with a hollow area (Subsector "c", Figure 5), which shows extensive recent gully and rill incisions, affecting a rather large portion of the slope, less than 20 m from the main road.

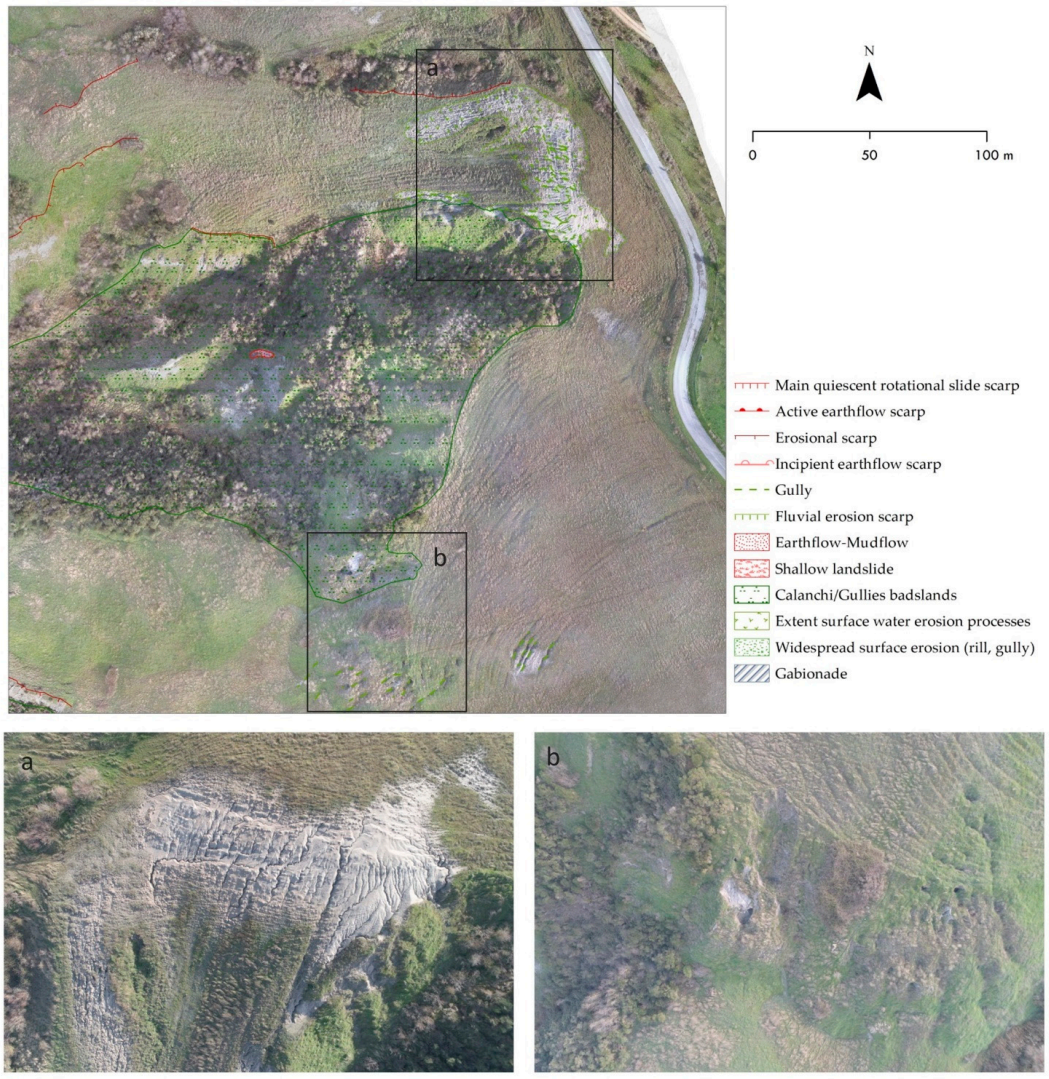


Figure 12. Local-scale geomorphological mapping derived from the visual inspection of the May 2024 UAV orthoimage, corresponding to (**a**) the calanchi area in neo-formation, close to the Provincial Road of Monte Amiata, close to Poggio Bandelli farm, with (**b**) some detail of rill and gully incisions and tunnel erosion identified.

4. Discussion

The need for new approaches for the description of geomorphological processes and the representation of landforms, whose spatial and temporal distribution represents the most immediate tool to detect areas affected by geological risks, is in increasing demand for territorial planning and for both local actions and management decisions. The production of multi-scale digital cartography models, characterized by a full-coverage representation of landforms, allows the provision of a complete and flexible representation of the complexity of the physical landscape's evolution. In this work, by pursuing the goal of modernizing the creation of geomorphological maps, the implemented approach addresses this need for the recognition and classification of landforms and the creation of multi-scale digital geomorphological maps. This approach was tested in a pilot Italian case in the Apennines, which share common pressing environmental challenges, such as gravitational and running water-based processes, which are commonly the cause of severe damage and implications for human life.

The slope-scale investigation based on 3D model LiDAR-derived regional data led to a portrayal of the main common landform types acting within the catchment. As

widely demonstrated in the literature [44,45,62] geomorphic-based landform classification represents an effective approach to delineate the main geomorphological elements of a territory. Also, compared with other ALCs based on moving window neighborhood analysis, the applied Geomorphons approach was demonstrated to be more flexible [44,45]. The analysis window, in fact, is based on the surrounding of a target cell imposed via search distance parameter setting, specifying where the area extends. Several studies have demonstrated the applicability of Geomorphons in diverse physiographic contexts, e.g., coastal [45], alpine [44], and basin scale [38], and contexts such as geology, urban planning [63], and archeology [64], providing a basic tool for a large-scale representation of the principal landforms of landscape useful for subsequent investigation at local scale, also considering the input DTM resolution. The availability of LiDAR products with metric resolution, as in the case of the investigated area, surely guarantees a reliable recognition of landform classes at different scales and spatial resolutions, being more limited for more coarse digital terrain models.

Simultaneously, the multi-temporal analysis of time-series of historical orthoimages allowed a characterization of the evolution of areas subjected to active movements. Geomorphological landform and landslide recognition by orthophoto inspection is a well-established method in the literature [65,66], mainly based on the photointerpretation of aerial photos or LiDAR-derived images. These inventories allow the accurate definition of the spatial and temporal distribution of landforms, facilitating a map that documents the typology and the extent of the observed phenomena—an essential element to a proper landscape evolution investigation—and an assessment of their interference with anthropic elements. The large number of images available makes it possible to recognize the diverse generation of landslides over an observed period, allowing an identification of the areas most frequently subject to gravitative and/or widespread erosion processes and a reconstruction of their morpho-evolution history [67,68] and their interrelation with the calanchi area. To consider how the availability of historical imagery over the Italian territory may, conversely, represent a limitation for more remote and less populous areas with no or significantly less image availability represents a potential limit in temporal-evolution characterization of other territory. In Apennine territories such as the one investigated, the rapid and persistent evolution of these landscapes over time has caused an accelerated rate of soil erosion [69,70], besides a close relationship between erosional and depositional processes over time [71], as mainly observed in the south-facing calanchi areas affected by a high recurrence of mud- and earthflows. This is less evident in the north-facing calanchi areas. Moreover, the large mass movements show a clear dismanteling by rills, gullies, and calanchi erosional processes. A significant interference with croplands has also been observed, mainly due to the retrogressive trend of the steepest badland areas. For that reason, in this territory, agricultural areas are constantly levelled and re-shaped by man-made intervention, to counter and limit the soil erosion effect of the badlands, which is a more complex operation in areas where croplands border the steepest calanchi areas [72]. The slope aspect contributes to the maintenance of the calanchi landforms: the southern exposure, accentuating arid conditions, in fact allows preservation of the steep slopes typical of calanchi, compared with those facing north [73]. In those areas with a high recurrence of active processes, evident in rapid destructive landslides or typical soil erosion along recurrent drainage lines by surface water runoff, a detailed geomorphological analysis may be important mainly for a local investigation of these processes and their potential interaction with anthropic elements.

UAV surveys provide very-high-resolution products; however, they are affected by operational limitations such as battery duration or restrictions (e.g., maximum flying height, no fly zones, etc. [74]). Moreover, for the optimal execution of a flight, the weather

conditions must be checked carefully. The very-high-resolution DEMs and orthoimages led to a focus on the most active and recurrent landforms, enabling the recognition and characterization of the most active sectors of an investigated area, via a geomorphological mapping at local scale. The recognized widespread runoff erosion processes testify to a territory highly subjected to intense erosion processes, confirming the rapid evolution of this territory over time. The persistence of gully and rill incision, as well as of extended badlands characterized by dense alternation of narrow V-shaped valleys with typical knife-edges, often associated with localized slope instabilities, favors an accelerated rate of soil erosion, mainly due to the high erodibility of the Plio-Pleistocene clays, attributable to physical and chemical properties of this sediments on contact with water [75]. Of high interest is the neo-formation of badlands, located in correspondence with a slight change of slope, potentially affecting the provincial road. As described in the literature [76] a typical badland-initiation pattern corresponds to an expansion of hillslope gullies in mid-slope, where local erosive runoff power overcomes soil-vegetation resistance. This trend is the product of a complex evolution of the territory, balanced between natural soil erosion processes and human intervention. Reclamation processes have been common in the Apennine territory, attributable to the socio-economic pressure of the 1950s, during which the badland areas were modelled to maximize the total hectares in cultivation [77,78]. The investigation of historical orthophotos highlighted that an area previously recognized as the initial badland area is viewable in 1988–89 images, then completely reclaimed for arable land (1994–98 images). In the following years, a gradual transition from arable land to grassland is observable, testifying to the recurrence and persistence of rill and gully incision occurrence over time.

5. Conclusions

A completely remote geomorphological mapping approach, based on a combination of multi-source data, considering primarily the increasing number of regional spatial data available and ad hoc UAV-derived products, was implemented. The proposed methodology was tested on a hilly landscape in the Central Apennine territories, in the southern portion of Tuscany, in Siena Province, characterized by a wide range of processes, mainly represented by erosive landforms, such as rills, gullies, and badlands, and a diverse type of gravitative processes. The methodology provided a tool to obtain a full-coverage representation of landforms and a multi-scale digital cartographic model with scalable geomorphological maps of a territory. Leveraging multi-source datasets having different resolutions, a map incorporating different hierarchical levels facilitated the making available of a complete and flexible representation of the complexity of the physical landscape's evolution; when feasible, a comparison with previously available datasets proved the reliability of the used algorithms. The proposed methodology guarantees a completely remote mode of landscape characterization, representing a suitable and key instrument for technicians and decision-makers in every action and decision on a territory, from land planning to civil engineering applications.

Author Contributions: Conceptualization, M.C. and D.G.; data curation, M.C., D.G., D.F.T. and M.B.; formal analysis, D.G. and D.F.T.; methodology, M.C., D.G. and M.B.; project administration, M.C.; supervision, M.C.; validation, M.C. and D.G.; visualization, M.C. and D.G.; writing—original draft, M.C. and D.G.; writing—review and editing, D.G., D.F.T. and M.B. All authors have read and agreed to the published version of the manuscript.

Funding: This research was funded and carried out in the Project FORMATION—Full cOveRage, Multi-scAle and multi sensor geomorphological map: a practical tool for TerritOrial plaNning—Progetto 2022C2XPK7_PE10_PRIN2022—PNRR M4.C2.1.1—Finanziato dall'Unione Europea—Next Generation EU—CUP: B53D23007010006.

Data Availability Statement: The Digital Terrain Model: source of data Tuscany Region—"LiDAR survey", free online, downloadable from the regional web Geo-Portal, i.e., GEOscopio (link: https://www.regione.toscana.it/-/geoscopio); Regional Geomorphological Database: source of data Tuscany Region—"DB Geomorfologico", free online, downloadable from the regional web Geo-Portal, i.e., GEOscopio (link: https://www.regione.toscana.it/-/geoscopio). Full and exclusive ownership of all these dataset rests with the Region of Tuscany, which authorizes the free consultation, extraction, reproduction, and modification of the data it contains in accordance with the terms of the user license under which it is released (License CC BY 4.0). URL (accessed on 8 March 2024).

Conflicts of Interest: The authors declare no conflicts of interest. The funders had no role in the design of the study; in the collection, analyses, or interpretation of data; in the writing of the manuscript; or in the decision to publish the results.

References

1. Lee, E.M. Geomorphological mapping. *Geol. Soc. Lond. Eng. Geol. Spec. Publ.* **2001**, *18*, 53–56. [CrossRef]
2. Evans, I.S. Geomorphometry and landform mapping: What is a landform? *Geomorphology* **2012**, *137*, 94–106. [CrossRef]
3. Dramis, F.; Guida, D.; Cestari, A. Nature and Aims of Geomorphological Mapping. *Dev. Earth Surf. Process.* **2011**, *15*, 39–73.
4. Turconi, L.; Tropeano, D.; Savio, G.; Bono, B.; De, S.K.; Frasca, M.; Luino, F. Torrential Hazard Prevention in Alpine Small Basin through Historical, Empirical and Geomorphological Cross Analysis in NW Italy. *Land* **2022**, *11*, 699. [CrossRef]
5. Seijmonsbergen, A.C.; De Graaff, L.W.S. Geomorphological mapping and geophysical profiling for the evaluation of natural hazards in an alpine catchment. *Nat. Hazards Earth Syst. Sci.* **2006**, *6*, 185–193. [CrossRef]
6. Cardinali, M.; Reichenbach, P.; Guzzetti, F.; Ardizzone, F.; Antonini, G.; Galli, M.; Cacciano, M.; Castellani, M.; Salvati, P. A geomorphological approach to the estimation of landslide hazards and risks in Umbria. *Nat. Hazards Earth Syst. Sci.* **2002**, *2*, 57–72. [CrossRef]
7. Pavlopoulos, K.; Evelpidou, N.; Vassilopoulos, A. *Mapping Geomorphological Environments*; Springer Science & Business Media: Berlin/Heidelberg, Germany, 2009.
8. Brunsden, D.; Doornkamp, J.C.; Fookes, P.G.; Jones, D.K.C.; Kelly, J.M.H. Large scale geomorphological mapping and highway engineering design. *Q. J. Eng. Geol. Hydrogeol.* **1975**, *8*, 227–253. [CrossRef]
9. Teixeira, J.; Chaminé, H.I.; Carvalho, J.M.; Pérez-Alberti, A.; Rocha, F. Hydrogeomorphological mapping as a tool in groundwater exploration. *J. Maps* **2013**, *9*, 263–273. [CrossRef]
10. Bufalini, M.; Materazzi, M.; De Amicis, M.; Pambianchi, G. From traditional to modern 'full coverage' geomorphological mapping: A study case in the Chienti river basin (Marche region, central Italy). *J. Maps* **2021**, *17*, 17–28. [CrossRef]
11. Sofia, G. Combining geomorphometry, feature extraction techniques and Earth-surface processes research: The way forward. *Geomorphology* **2020**, *355*, 107055. [CrossRef]
12. Viles, H. Technology and geomorphology: Are improvements in data collection techniques transforming geomorphic science? *Geomorphology* **2016**, *270*, 121–133. [CrossRef]
13. Lin, S.; Chen, N.; He, Z. Automatic landform recognition from the perspective of watershed spatial structure based on digital elevation models. *Remote Sens.* **2021**, *13*, 3926. [CrossRef]
14. Guzzetti, F. Landslide fatalities and the evaluation of landslide risk in Italy. *Eng. Geol.* **2000**, *58*, 89–107. [CrossRef]
15. Herrera, G.; Mateos, R.M.; García-Davalillo, J.C.; Grandjean, G.; Poyiadji, E.; Maftei, R.; Filipciuc, T.-C.; Jemec Auflič, M.; Jež, J.; Podolszki, L.; et al. Landslide databases in the Geological Surveys of Europe. *Landslides* **2018**, *15*, 359–379. [CrossRef]
16. Mateos, R.M.; López-Vinielles, J.; Poyiadji, E.; Tsagkas, D.; Sheehy, M.; Hadjicharalambous, K.; Liscák, P.; Podolski, L.; Laskowicz, I.; Iadanza, C.; et al. Integration of landslide hazard into urban planning across Europe. *Landsc. Urban Plan.* **2020**, *196*, 103740. [CrossRef]
17. Guzzetti, F.; Stark, C.P.; Salvati, P. Evaluation of Flood and Landslide Risk to the Population of Italy. *Environ. Manag.* **2005**, *36*, 15–36. [CrossRef] [PubMed]
18. De Jong, M.G.G.; Sterk, H.P.; Shinneman, S.; Seijmonsbergen, A.C. Hierarchical geomorphological mapping in mountainous areas. *J. Maps* **2021**, *17*, 214–225. [CrossRef]
19. Gustavsson, M.; Kolstrup, E.; Seijmonsbergen, A.C. A new symbol-and-GIS based detailed geomorphological mapping system: Renewal of a scientific discipline for understanding landscape development. *Geomorphology* **2006**, *77*, 90–111. [CrossRef]
20. Quesada-Román, A.; Peralta-Reyes, M. Geomorphological mapping global trends and applications. *Geographies* **2023**, *3*, 610–621. [CrossRef]
21. Godone, D.; Giordan, D.; Baldo, M. Rapid mapping application of vegetated terraces based on high resolution airborne lidar. *Geomat. Nat. Hazards Risk* **2018**, *9*, 970–985. [CrossRef]

22. Baldo, M.; Bicocchi, C.; Chiocchini, U.; Giordan, D.; Lollino, G. LIDAR monitoring of mass wasting processes: The Radicofani landslide, Province of Siena, Central Italy. *Geomorphology* **2009**, *105*, 193–201. [CrossRef]
23. Jaboyedoff, M.; Oppikofer, T.; Abellán, A.; Derron, M.-H.; Loye, A.; Metzger, R.; Pedrazzini, A. Use of LIDAR in landslide investigations: A review. *Nat. Hazards* **2012**, *61*, 5–28. [CrossRef]
24. Cavalli, M.; Marchi, L. Characterisation of the surface morphology of an alpine alluvial fan using airborne LiDAR. *Nat. Hazards Earth Syst. Sci.* **2008**, *8*, 323–333. [CrossRef]
25. Gentili, F.; Madonna, S. Photogrammetry from UAV and Low-Cost Lidar for Sinkhole Hazard Mitigation in Urban Areas: Applications and Evaluations. *Geographies* **2024**, *4*, 343–362. [CrossRef]
26. Neugirg, F.; Stark, M.; Kaiser, A.; Vlacilova, M.; Della Seta, M.; Vergari, F.; Schmidt, J.; Becht, M.; Haas, F. Erosion processes in calanchi in the Upper Orcia Valley, Southern Tuscany, Italy based on multitemporal high-resolution terrestrial LiDAR and UAV surveys. *Geomorphology* **2016**, *269*, 8–22. [CrossRef]
27. Godone, D.; Allasia, P.; Borrelli, L.; Gullà, G. UAV and structure from motion approach to monitor the maierato landslide evolution. *Remote Sens.* **2020**, *12*, 1039. [CrossRef]
28. Cignetti, M.; Godone, D.; Wrzesniak, A.; Giordan, D. Structure from Motion Multisource Application for Landslide Characterization and Monitoring: The Champlas du Col Case Study, Sestriere, North-Western Italy. *Sensors* **2019**, *19*, 2364. [CrossRef]
29. Tarolli, P. High-resolution topography for understanding Earth surface processes: Opportunities and challenges. *Geomorphology* **2014**, *216*, 295–312. [CrossRef]
30. Passalacqua, P.; Belmont, P.; Staley, D.M.; Simley, J.D.; Arrowsmith, J.R.; Bode, C.A.; Crosby, C.; DeLong, S.B.; Glenn, N.F.; Kelly, S.A.; et al. Analyzing high resolution topography for advancing the understanding of mass and energy transfer through landscapes: A}review. *Earth-Sci. Rev.* **2015**, *148*, 174–193. [CrossRef]
31. Minár, J.; Evans, I.S. Elementary forms for land surface segmentation: The theoretical basis of terrain analysis and geomorphological mapping. *Geomorphology* **2008**, *95*, 236–259. [CrossRef]
32. Tarolli, P.; Dalla Fontana, G. Hillslope-to-valley transition morphology: New opportunities from high resolution DTMs. *Geomorphology* **2009**, *113*, 47–56. [CrossRef]
33. Anders, N.S.; Seijmonsbergen, A.C.; Bouten, W. Segmentation optimization and stratified object-based analysis for semi-automated geomorphological mapping. *Remote Sens. Environ.* **2011**, *115*, 2976–2985. [CrossRef]
34. Weiss, A. Topographic position and landforms analysis. In Proceedings of the Poster Presentation, ESRI User Conference, San Diego, CA, USA, 9–13 July 2001; Volume 200.
35. Jasiewicz, J.; Stepinski, T.F. Geomorphons—A pattern recognition approach to classification and mapping of landforms. *Geomorphology* **2013**, *182*, 147–156. [CrossRef]
36. Shirani, K.; Solhi, S.; Pasandi, M. Automatic Landform Recognition, Extraction, and Classification using Kernel Pattern Modeling. *J. Geovis. Spat. Anal.* **2023**, *7*, 2. [CrossRef]
37. Tagil, S.; Jenness, J. GIS-based automated landform classification and topographic, landcover and geologic attributes of landforms around the Yazoren Polje, Turkey. *J. Appl. Sci.* **2008**, *8*, 910–921. [CrossRef]
38. Khan, A.; Govil, H. Evaluation of potential sites for soil erosion risk in and around Yamuna River flood plain using RUSLE. *Arab. J. Geosci.* **2020**, *13*, 707. [CrossRef]
39. Crema, S.; Cavalli, M. SedInConnect: A stand-alone, free and open source tool for the assessment of sediment connectivity. *Comput. Geosci.* **2018**, *111*, 39–45. [CrossRef]
40. van Asselen, S.; Seijmonsbergen, A.C. Expert-driven semi-automated geomorphological mapping for a mountainous area using a laser DTM. *Geomorphology* **2006**, *78*, 309–320. [CrossRef]
41. Cavalli, M.; Tarolli, P.; Marchi, L.; Dalla Fontana, G. The effectiveness of airborne LiDAR data in the recognition of channel-bed morphology. *Catena* **2008**, *73*, 249–260. [CrossRef]
42. Tarolli, P.; Sofia, G.; Dalla Fontana, G. Geomorphic features extraction from high-resolution topography: Landslide crowns and bank erosion. *Nat. Hazards* **2012**, *61*, 65–83. [CrossRef]
43. Kramm, T.; Hoffmeister, D.; Curdt, C.; Maleki, S.; Khormali, F.; Kehl, M. Accuracy Assessment of Landform Classification Approaches on Different Spatial Scales for the Iranian Loess Plateau. *ISPRS Int. J. Geo-Inf.* **2017**, *6*, 366. [CrossRef]
44. Gruber, F.E.; Baruck, J.; Geitner, C. Algorithms vs. surveyors: A comparison of automated landform delineations and surveyed topographic positions from soil mapping in an Alpine environment. *Geoderma* **2017**, *308*, 9–25. [CrossRef]
45. Gioia, D.; Danese, M.; Corrado, G.; Di Leo, P.; Minervino Amodio, A.; Schiattarella, M. Assessing the Prediction Accuracy of Geomorphon-Based Automated Landform Classification: An Example from the Ionian Coastal Belt of Southern Italy. *ISPRS Int. J. Geo-Inf.* **2021**, *10*, 725. [CrossRef]
46. Mokarram, M.; Sathyamoorthy, D. A review of landform classification methods. *Spat. Inf. Res.* **2018**, *26*, 647–660. [CrossRef]
47. Wieczorek, M.; Migoń, P. Automatic relief classification versus expert and field based landform classification for the medium-altitude mountain range, the Sudetes, SW Poland. *Geomorphology* **2014**, *206*, 133–146. [CrossRef]

48. La Licata, M.; Bosino, A.; Bettoni, M.; Maerker, M. Assessing landscape features and geomorphic processes influencing sediment dynamics in a geomorphologically highly active Mediterranean agroecosystem: The upper Val d'Arda case study (Northern Apennines, Italy). *Geomorphology* **2023**, *433*, 108724. [CrossRef]
49. Gioia, D.; Bavusi, M.; Di Leo, P.; Giammatteo, T.; Schiattarella, M. Geoarchaeology and geomorphology of the Metaponto area, Ionian coastal belt, Italy. *J. Maps* **2020**, *16*, 117–125. [CrossRef]
50. Vergari, F.; Della Seta, M.; Del Monte, M.; Fredi, P.; Lupia Palmieri, E. Landslide susceptibility assessment in the Upper Orcia Valley (Southern Tuscany, Italy) through conditional analysis: A contribution to the unbiased selection of causal factors. *Nat. Hazards Earth Syst. Sci.* **2011**, *11*, 1475–1497. [CrossRef]
51. Tuscany Region GeoScopio. Available online: https://www.regione.toscana.it/-/geoscopio (accessed on 21 June 2024).
52. Stepinski, T.F.; Jasiewicz, J. Geomorphons-a new approach to classification of landforms. *Proc. Geomorphometry* **2011**, *2011*, 109–112.
53. Conrad, O.; Bechtel, B.; Bock, M.; Dietrich, H.; Fischer, E.; Gerlitz, L.; Wehberg, J.; Wichmann, V.; Böhner, J. System for automated geoscientific analyses (SAGA) v. 2.1. 4. *Geosci. Model Dev.* **2015**, *8*, 1991–2007. [CrossRef]
54. QGIS Development Team. *QGIS Geographic Information System*; Open Source Geospatial Foundation: Beaverton, OR, USA, 2024.
55. R Development Core Team. *R: A Language and Environment for Statistical Computing*; Team, R.D.C., Ed.; R Foundation for Statistical Computing: Vienna, Austria, 2022; Volume 1, ISBN 3-900051-07-0.
56. Ministero dell'ambiente e della Sicurezza Energetica Portale Cartografico Nazionale. Available online: https://gn.mase.gov.it/portale/home (accessed on 21 June 2024).
57. Migoń, P.; Kacprzak, A.; Malik, I.; Kasprzak, M.; Owczarek, P.; Wistuba, M.; Pánek, T. Geomorphological, pedological and dendrochronological signatures of a relict landslide terrain, Mt Garbatka (Kamienne Mts), SW Poland. *Geomorphology* **2014**, *219*, 213–231. [CrossRef]
58. Fiorucci, F.; Giordan, D.; Santangelo, M.; Dutto, F.; Rossi, M.; Guzzetti, F. Criteria for the optimal selection of remote sensing optical images to map event landslides. *Nat. Hazards Earth Syst. Sci* **2018**, *18*, 405–417. [CrossRef]
59. Cruden, D.M.; Varnes, D.J. Landslides Types and Processes. In *Landslides: Investigation and Mitigation*; Turner, A.K., Schuster, R.L., Eds.; Transportation Research Board Special Report 247; National Academy Press: Washington, DC, USA, 1996; pp. 36–75.
60. Hungr, O.; Leroueil, S.; Picarelli, L. The Varnes classification of landslide types, an update. *Landslides* **2014**, *11*, 167–194. [CrossRef]
61. ISPRA Serv. Geol. Italia Aggiornamento ed integrazioni delle Linee Guida della Carta Geomorfologica d'Italia alla Scala 1:50000. *Quad. Ser. III* **2018**, *13*, 93.
62. Vannametee, E.; Babel, L.V.; Hendriks, M.R.; Schuur, J.; De Jong, S.M.; Bierkens, M.F.P.; Karssenberg, D. Semi-automated mapping of landforms using multiple point geostatistics. *Geomorphology* **2014**, *221*, 298–319. [CrossRef]
63. Manfré, L.A.; de Albuquerque Nóbrega, R.A.; Quintanilha, J.A. Regional and local topography subdivision and landform mapping using SRTM-derived data: A case study in southeastern Brazil. *Environ. Earth Sci.* **2015**, *73*, 6457–6475. [CrossRef]
64. Verhagen, P.; Druaguct, L. Object-based landform delineation and classification from DEMs for archaeological predictive mapping. *J. Archaeol. Sci.* **2012**, *39*, 698–703. [CrossRef]
65. Guzzetti, F.; Mondini, A.C.; Cardinali, M.; Fiorucci, F.; Santangelo, M.; Chang, K.-T. Landslide inventory maps: New tools for an old problem. *Earth Sci. Rev.* **2012**, *112*, 42–66. [CrossRef]
66. Santangelo, M.; Zhang, L.; Rupnik, E.; Deseilligny, M.P.; Cardinali, M. Landslide Evolution Pattern Revealed by Multi-Temporal Dsms Obtained from Historical Aerial Images. In Proceedings of the ISPRS Congress, Nice, France, 6–11 June 2022; Volume 43, pp. 1085–1092.
67. Bucci, F.; Santangelo, M.; Fiorucci, F.; Ardizzone, F.; Giordan, D.; Cignetti, M.; Notti, D.; Allasia, P.; Godone, D.; Lagomarsino, D.; et al. Geomorphologic landslide inventory by air photo interpretation of the High Agri Valley (Southern Italy). *J. Maps* **2021**, *17*, 376–388. [CrossRef]
68. Ardizzone, F.; Bucci, F.; Cardinali, M.; Fiorucci, F.; Pisano, L.; Santangelo, M.; Zumpano, V. Geomorphological landslide inventory map of the Daunia Apennines, southern Italy. *Earth Syst. Sci. Data* **2023**, *15*, 753–767. [CrossRef]
69. Ciccacci, S.; Galiano, M.; Roma, M.A.; Salvatore, M.C. Morphological analysis and erosion rate evaluation in badlands of Radicofani area (Southern Tuscany—Italy). *Catena* **2008**, *74*, 87–97. [CrossRef]
70. Aucelli, P.P.C.; Conforti, M.; Della Seta, M.; Del Monte, M.; D'uva, L.; Rosskopf, C.M.; Vergari, F. Multi-temporal digital photogrammetric analysis for quantitative assessment of soil erosion rates in the Landola catchment of the Upper Orcia Valley (Tuscany, Italy). *L. Degrad. Dev.* **2016**, *27*, 1075–1092. [CrossRef]
71. Vergari, F.; Troiani, F.; Faulkner, H.; Del Monte, M.; Della Seta, M.; Ciccacci, S.; Fredi, P. The use of the slope--area function to analyse process domains in complex badland landscapes. *Earth Surf. Process. Landforms* **2019**, *44*, 273–286. [CrossRef]
72. Vergari, F.; Della Seta, M.; Del Monte, M.; Barbieri, M. Badlands denudation "hot spots": The role of parent material properties on geomorphic processes in 20-years monitored sites of Southern Tuscany (Italy). *Catena* **2013**, *106*, 31–41. [CrossRef]
73. Vergari, F. Assessing soil erosion hazard in a key badland area of Central Italy. *Nat. Hazards* **2015**, *79*, 71–95. [CrossRef]

74. Giordan, D.; Adams, M.S.; Aicardi, I.; Alicandro, M.; Allasia, P.; Baldo, M.; De Berardinis, P.; Dominici, D.; Godone, D.; Hobbs, P.; et al. The use of unmanned aerial vehicles (UAVs) for engineering geology applications. *Bull. Eng. Geol. Environ.* **2020**, *79*, 3437–3481. [CrossRef]
75. Phillips, C.P. The badlands of Italy: A vanishing landscape? *Appl. Geogr.* **1998**, *18*, 243–257. [CrossRef]
76. las Heras, M.; Gallart, F. The origin of badlands. In *Badlands Dynamics in a Context of Global Change*; Elsevier: Amsterdam, The Netherlands, 2018; pp. 27–59.
77. Phillips, C.P. Reclaiming the erosion susceptible landscape of the Italian badlands for arable cultivation. *Land Degrad. Dev.* **1998**, *9*, 331–346. [CrossRef]
78. Coratza, P.; Parenti, C. Controlling Factors of Badland Morphological Changes in the Emilia Apennines (Northern Italy). *Water* **2021**, *13*, 539. [CrossRef]

Disclaimer/Publisher's Note: The statements, opinions and data contained in all publications are solely those of the individual author(s) and contributor(s) and not of MDPI and/or the editor(s). MDPI and/or the editor(s) disclaim responsibility for any injury to people or property resulting from any ideas, methods, instructions or products referred to in the content.